Ab-initio study of the physical properties of $Zn_{1-x}Mg_xSe_yTe_{1-y}$quaternary alloy

Y.Megdoud[a,b]*, L.Tairi[b,c], R.Menaceur[d], N. Bourahla[a], S.Ghemid[b] and H.Meradji[b]
[a]Institute of Sciences, University Center of Tipaza- Morsli Abdallah-, Algeria
[b]LPR Laboratory, Département of Physics, Faculty of Science, Badji Mokhtar University, Annaba, Algeria.
[c]Research Center in Industrial Technologies CRTI, P.O. Box 64, Cheraga16014 Algiers Algeria
[d]Unite de Development des Energies Renouvelables dans les Zones Arides (UDERZA).

Correspondent author Email; Y.megdoud23@gmail.com
Received 04/2023; Accepted 06/2023; Published 08/2023

Abstract:

First-principles calculations are performed to study the structural, electronic and properties of **$Zn_{1-x}Mg_xSe_yTe_{1-y}$** alloys using the full potential-linearized augmented plane wave method (**FP-LAPW)** within the density functional theory**(DFT).**In this approach the Perdew-Burke-Ernzerhorf generalized gradient approximation (PBE-GGA) was used for the exchange-correlation potential. Moreover, the modified Becke Johnson approximation **(mBJ)** was also used for band structure calculations. Firstly we studied the **MgX** binary compounds. The lattice constant for the ternary alloys exhibits a small deviation from the Vegard's law. The microscopic origins of the gap bowing were explained by using the approach of Zunger and co-workers. The bowing of the fundamental gap versus composition predicted by our calculations is in good agreement with available theoretical data. In addition, we have studied the thermal properties of these alloysusing the Debye model implemented in Gibbs program. Finally, the energy band gap of **$Zn_{1-x}Mg_xSe_yTe_{1-y}$** quaternary alloys lattice matched **to In As and ZnTe** substrats was investigated. To our knowledge this is the first quantitative theoretical investigation on **$Zn_{1-x}Mg_xSe_yTe_{1-y}$**quaternaryalloys and still awaits experimental confirmations.

Keywords: Quaternary alloys, Functional density(DFT), Approximation of the generalized gradient (PBE-GGA) ,mBJ approximation, InAs and ZnTe substrates.
DOI Number: 10.48047/nq.2023.21.6.NQ23144 NeuroQuantology2023;21(6): 1416-1428

1. Introduction

The optoelectronic properties of semiconductors have been the subject of intense research and technological interest in recent times due to their new applications. Type II-IV semiconductors are of practical interest because their field of application is very vast and all the devices of these semiconductors can be characterized and identified more or less precisely. Most **II-VI** semiconductors are characterized by a bandgap greater than 1eV. Wide bandgap **II-VI** semiconductors are suitable for applications such as laser diodes operating in the visible region of the spectrum, those with small bandgap prohibited are used in the manufacture of infrared detectors **[1].** applications in optoelectronics **[2]** and luminescent devices **[3].** These compounds can crystallize in several structures such as **NaCl** (B1), **zinc-blende** (B3), **wurtzite** (B4) and **NiAs**(B8) structure **[4].** These materials have been extensively studied experimentally and theoretically, however there are controversial data to about the structure and their ground state at high pressure due to the very small energy difference between the different phases that these materials adopt. Zinc selenide (**ZnSe**) and zinc telluride (**ZnTe**) are among the most important Group **II-VI** semiconductor materials due to their vast potential for applications in different

optoelectronic devices specifically laser diodes emitting carbon. Visible light and in the blue region of the spectrum. They are also widely used for their high efficiency in photovoltaic cells**[4].** The incorporation of the Mg element in compounds strongly affects the physical properties of these materials. The advantages of incorporating the latter are the strengthening of strongly ionic networks, with concomitant effects on the generation and propagation of defects, as well as the lifetime of the devices **[5-6].** A Mg-based blue-green laser containing II-VI semiconductors operating continuously at room temperature with a lifetime of more than 100 h has already been realized **[7].** Semiconductor II-VI alloys are used in optoelectronic devices, ranging from blue to near ultraviolet spectral region **[8]** and are also used for manufacture X-rays and detector ray **[9,10].** The ternary and quaternary alloys Zn_{1-x} $Mg_xSe_yTe_{1-y}$ where the element Mg is incorporated are very attractive. Theoretical and experimental studies have been carried out on the ternary alloys $Zn_{1-x}Mg_xSe$**[11],**Zn_{1-x} Mg_xTe**[12],** $ZnSe_xTe_{1-x}$**[13].** On the other hand, no theoretical or experimental work has been carried out on the physical properties of the ternary alloys MgSexTe1-x and the quaternary alloys $Zn_{1-x}Mg_xSe_yTe_{1-y}$ adapted to the **InAs** substrate. Therefore, our main goal of this work is to study the structural and electronic properties of $Zn_{1-x}Mg_xSe_yTe_{1-y}$ alloys by using first-principles calculations to gain better insight into these technologically promising materials. The organization of this article is as follows. In **Section 2** we briefly describe the computational method used in this work. Results will be presented and discussed in **Section 3**. A summary of the work will be given in **Section 4.**

2. Computational details and theoretical background

The calculations were performed using the full-potential linearized augmented plane wave **(FPLAPW**) method **[14]** within the frame work of the**DFT[15,16]** as implemented in the WIEN2K code **[17],** which is one of the most efficient method of simulating and calculating the ground state properties of cyrstalline materials **[18].** The exchange-correlation potential for the structural properties was calculated by the generalized gradient approximation (GGA) based on Perdew et al. **[19],** while for the electronic properties, the Becke-Johnson (Mbj) scheme **[20]** was applied. In the **FP-LAPW** method, the wave function, charge density and potential are expanded differently in two regions of the unit cell. Inside the non-overlapping spheres around each atom of radius RMT (muffin-tin radius), spherical harmonic expansion is used and in the remaining space of the unit cell, a plane wave basis set is chosen. The convergence parameter,$R_{MT}k_{max}$which controls the size of the basis sets in these calculations, was set to 8. RMT denotes the smallest atomic sphere radius and **kmax** gives the magnitude of the largest k vector in the plane wave expansion. The charge density was Fourier expanded up to **Gmax = 14 (Ryd)1/2** and the maximum l quantum number for the wave function expansion inside the atomic spheres was confined to **lmax = 10.** The muffin-tin radius was assumed to be **2.3,2.0, 2.0, 2.2 and 2.0** atomic units (a.u.) for the**Zn**, **Mg**, **S, Se** and **Te**atoms, respectively. A mesh of **47** special k-points for these binary compounds was taken in the irreducible wedge of the Brillouin zone. Both the plane wave cut-off and the number of k-points were varied to ensure total energy convergence.

3. Results and Discussion

3.1. Binary compounds

The quaternary system, studied in this article, is delimited by four ternary systems: **ZnSeyTe1-y,MgSeyTe1-y, Zn1-xMgxSe and Zn1-xMgxTe.** Then these pseudo-binary (ternary) alloys are in turn made of four binary compounds **MgSe, MgTe, ZnSe and ZnTe.** Therefore, as a starting point, we calculated the structural properties of binary compounds in the Zinc-blende structure using the WC-GGA scheme. The calculated total energies at many different volumes around equilibrium were fitted by Murnaghan's equation of state **[21],** to obtain the equilibrium lattice constant and Compressibility modulus for binary compounds. The results obtained for these binary compounds are given in **Table 1.** Our results agree well with the available

experimental and theoretical data. Calculated band structures of binary compounds using both WC-GGA and mBj schemes indicate a direct Γ→Γ band gap for **ZnSe and ZnTe. MgSe** and **MgTe** binary compounds. The results of our calculated band gaps are listed in **Table 2.** We see that our calculated WC-GGA bandgap energies are underestimated. In fact, WC-GGA generally underestimates the experimental energy bandgap; this is an intrinsic feature of the DFT which is not suitable for describing the properties of the excited state. However, it is widely accepted that the GGA electronic band structures are qualitatively in good agreement with the experiments with respect to the order of the energy levels and the shape of the bands. **Becke and Johnson** considering this deficiency in the energy gap constructed a new functional form of the GGA which is able to better reproduce the exchange potential at the cost of less agreement in the exchange energy. This approach gives better band separation. However, in this method gives values comparable to those of the experimental and takes into account the excited states. **Ex** such as the equilibrium volumes and the compressibility modulus are in bad agreement with the experiment. Therefore, in order to obtain more accurate energy bandgaps in our calculations.

Table 1 : Lattice parameters (in Å), bulk modulus (in GPa), its pressure derivative for ZnSe , MgSe, MgTe and ZnTe compounds

Lattice parameter a_0(A^0)			compressibility ModullusB_0(GPa)		
Compounds	**Our calculation**	**Exp**	**Others calculs**	**Our calculation**	**Exp**	**Others calculs**
ZnSe	**5.753**	**5.668[a]**	**5.635[a], 5.666[d]**	**57.108**	**64.7[e]**	**63.9[f], 67.32[d]**
ZnTe	**6.208**	**6.103[a]**	**6.074[a], 6.198[b], 6.054[c]**	**43.537**	**50.9[j]**	**51.75[c], 47.7[k]**
MgSe	**5.998**	**5.89[l]**	**5.88[m], 6.02[C]**	**44.445**	**-**	**50.5[m], 48.1[c]**
MgTe	**6.512**	**6.39[O]**	**6.38[P], 6.44[q]**	**33.519**	**38.0[O]**	**38.7[P], 38.0[q]**

[a]Ref[28],[b]Ref[29],[c]Ref[30], [d]Ref[31], [e]Ref[32],[f]Ref[33],[j]Ref[34], [k]Ref[35], [l][36], [m][37],[O][38][P][39] and [q][40].

Table 2: Energy gaps of the binary compounds MgSe, MgTe, ,ZnSe and ZnTe (in eV).

Γ-Γ	**Present Work**		**Exp**	**Other calculations**
	GGA	**mBJ**		
ZnSe	0.934	2.583	2.68[c]	1.863[d], 1.848[b], 2.50[e]
ZnTe	0.865	2.171	2.28[f]	1.57[a], 2.10[g], 1.01[a]
MgSe	2.551	4.262	3.6[f], 2.47[g],	2.825[c], 2.56[d], 3.90[e]
MgTe	2.325	3.667	2.29[g], 3.67[i]	2.615[c],2.32[d], 2.50[j] 0.414[c],

[a]Ref[39],[b]Ref[33]; [c]Ref[30], [d]Ref[41], [e]Ref[42], [f]Ref[43], [g]Ref[44].

3.2. Ternary alloys

The structural and electronic properties of pseudobinary (ternary) alloys **$ZnSe_yTe_{1-y}$, $MgSe_yTe_{1-y}$, $Zn_{1-x}Mg_xSe$ and $Zn_{1-x}Mg_xTe$** have been studied in the second step of our investigation. We have used ordered structures described in terms of supercells with eight atoms per unit cell, for the

compositions **x = 0.25, 0.5 and 0.75**. For the considered structures, we performed the structural optimization by minimizing the total energy with respect to the cell parameters and the atomic positions. Our calculated lattice constants at different composition of **$ZnSe_yTe_{1-y}$, $Zn_{1-x}Mg_xSe$ and $Zn_{1-x}Mg_xTe$** alloys, as shown in **Fig. 1**, were found to vary almost linearly with concentration following the Vegard's law **[22],** we calculated the disorder factor (bowing) of the network parameter, using the following form:

$$a(A_xB_{1-x}C)=xa_{AC}+(1-x)a_{BC} - bx(1-x) \quad (1)$$

Where$a_{AC}$and $a_{BC}$are the equilibrium lattice parameters for compounds AC and BC respectively. The disorder parameters (bowing) of the ternary alloysof **$ZnSe_yTe_{1-y}$, $Zn_{1-x}Mg_xSe$ and $Zn_{1-x}Mg_xTe$**have the following values:

: -0.451Å, , 0.256Å (0.34Å [23],0.40Å[24]), 0.31 Å(0.56[23] Å, 0.60[25])respectively. This deviation is due to the difference between the lattice parameters of the binary parent compounds **ZnSe, ZnTe, MgSe and MgTe**. On the other hand, the modulus of compressibility for**$ZnSe_yTe_{1-y}$,$MgSe_yTe_{1-y}$, $Zn_{1-x}Mg_xSe$ and $Zn_{1-x}Mg_xTe$** shows a deviation from linearity (bowing). (**See Fig 2**) , was observed. A more precise comparison of the behaviors of these ternary alloys shows that the decrease of the lattice constant is accompanied by the increase of the bulk modulus. It represents bond strengthening or weakening effects induced by changing the composition. The physical origin of this deviation should be mainly due to the mis matches of the bulk modulus of the binary compounds.

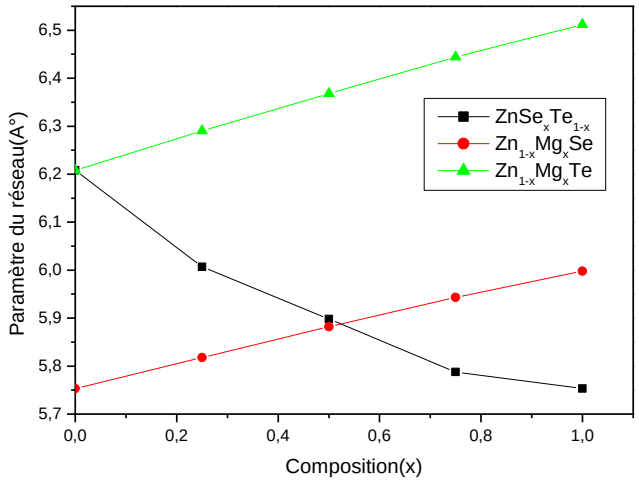

Fig 1: Lattice parameter variation of concentration x for ternary alloys **$ZnSe_yTe_{1-y}$,$Zn_{1-x}Mg_xSe$ and $Zn_{1-x}Mg_xTe$**.

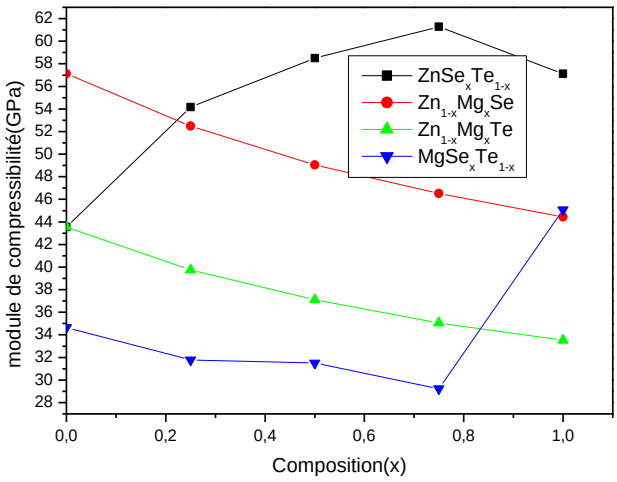

Fig 2: compressibility modulus as a function of concentration x for the ternary alloys **$ZnSe_yTe_{1-y}$,$MgSe_yTe_{1-y}$, $Zn_{1-x}Mg_xSe$ and $Zn_{1-x}Mg_xTe$.**

The study of the electronic properties of the ternary alloys of **$ZnSe_yTe_{1-y}$,$MgSe_yTe_{1-y}$, $Zn_{1-x}Mg_xSe$ and $Zn_{1-x}Mg_xTe$**. For these alloys, the band structures have been calculated along the high symmetry directions in the first Brillouin zone. The calculations were performed using the equilibrium Lattice parameters optimized in our previous calculations. The results obtained for the concentrations **x= 0.25, 0.5 and 0.75** are collated in **The table (3).**It should be noted that the gaps calculated for the **$ZnSe_yTe_{1-y}$,$MgSe_yTe_{1-y}$, $Zn_{1-x}Mg_xSe$ and $Zn_{1-x}Mg_xTe$**alloys are direct in the direction→By comparing our results with the data available in the literature, it appears from **Table 3** that the values of the gaps calculated by our method are in very good agreement with other published works using the approximation (PBE-GGA). We have illustrated the evolution of the energy gap of our ternary alloys with the concentration x in **Fig 3**, this is done for the two **mBJ et PBE-GGA** approximations. The disorder parameter of each alloy was calculated by fitting the curve of the variation of the gap as a function of the concentration to a quadratic function, the gap takes the following form:

$$E_g^{ABC} = xE_g^{BC} + (1-x)E_g^{AC} - bx(1-x) \qquad (2)$$

$ZnSe_yTe_{1-y}$:
$$E_g^{PBE-GGA} = 0.887 + 1.157X - 1.122X^2$$
$$E_g^{mBj} = 2.170 + 1.432X - 1.002X^2$$

$Zn_{1-x}Mg_xSe$:
$$E_g^{PBE-GGA} = 0.986 + 1.008X - 0.502X^2$$
$$E_g^{mBj} = 2.646 + 0.475X - 1.066X^2$$

$Zn_{1-x}Mg_xTe_x$:
$$E_g^{PBE-GGA} = 0.921 - 0.542X + 0.793X^2$$
$$E_g^{mBj} = 2.255 - 0.340X + 1.650X^2$$

$MgSe_yTe_{1-y}$:
$$E_g^{PBE-GGA} = 2.198 - 4.613X + 4.266X^2$$

$$E_g^{mBj} = 3.672 - 11.198X + 11.342X^2$$

Table 3: Energy gaps of alloys **$ZnSe_xTe_{1-x}$, Zn1-xMg_xSe, $Zn_{1-x}Mg_xTe$ and $MgSe_xTe_{1-x}$** calculated by PBE-GGA and mBJ, and compared to other theoretical values.

		E_g (eV) Γ- Γ			
Alloys	**X**	**Our calculation CCA mBj**		**Exp**	**Others calculs**
$ZnSe_xTe_{1-x}$	**0.25**	**1.164**		**-**	**1.457[a]**
	0.5	**2,480**		**-**	**1.448[a]**
	0.75	**1.151**		**-**	**1.545[a]**
		2.587			
		1.114			
		2.731			
Zn1-xMg_xSe	**0.25**	**1.375**		**-**	**1.427[b], 2,060[b]**
	0.5	**2.951**	**1,68**	**-**	**1.710 [b], 2.512 [b]**
	0.75	**3.17**	**1,919**	**-**	**2.027[b], 2.857[b]**
		3,448			
$Zn_{1-x}Mg_xTe$	**0.25**	**1,207**		**-**	**1.253[c], 1,827[c]**
	0.5	**1,625**		**-**	**1.45 6[c], 2.039[c]**
	0.75	**1.427**		**-**	**1.687[c], 2.70[c]**
		2,550	**1,625**		
		2.707			
$MgSe_xTe_{1-x}$	**0.25**	**1.567**		**-**	**-**
	0.5	**1.676**		**-**	**-**
	0.75	**1.621**		**-**	**-**
		1.635	**0. 334**		
		0.591			

[a]Ref[45],[b]Ref[36], [c]Ref[46].

The coefficients of the quadratic terms in these equations are the disorder parameters of the energy gaps of our alloys. The results for the disorder parameter using mBJ for the alloys **$ZnSe_yTe_{1-y}$,$MgSe_yTe_{1-y}$, $Zn_{1-x}Mg_xSe$ and $Zn_{1-x}Mg_xTe$** are **1.342, -1.002, 1.066, 1.650** respectively.

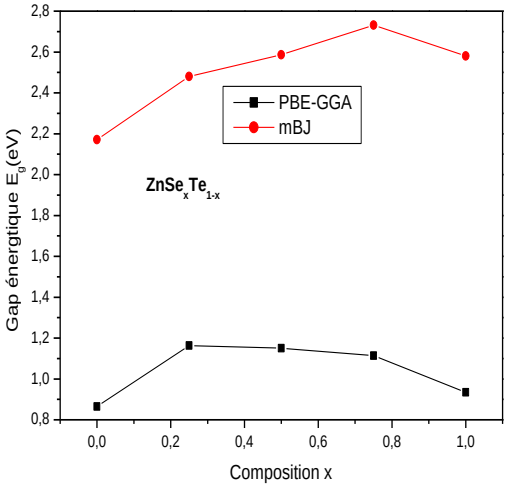

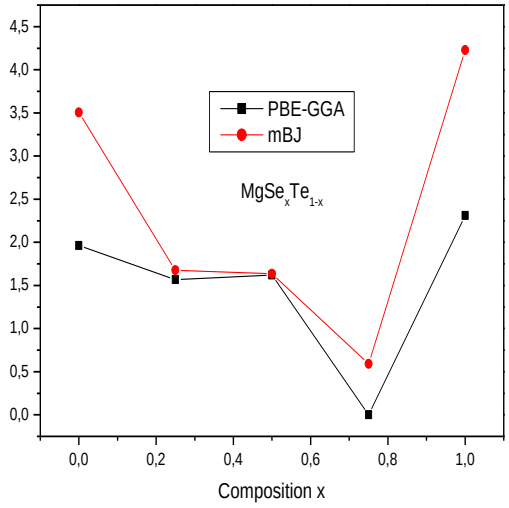

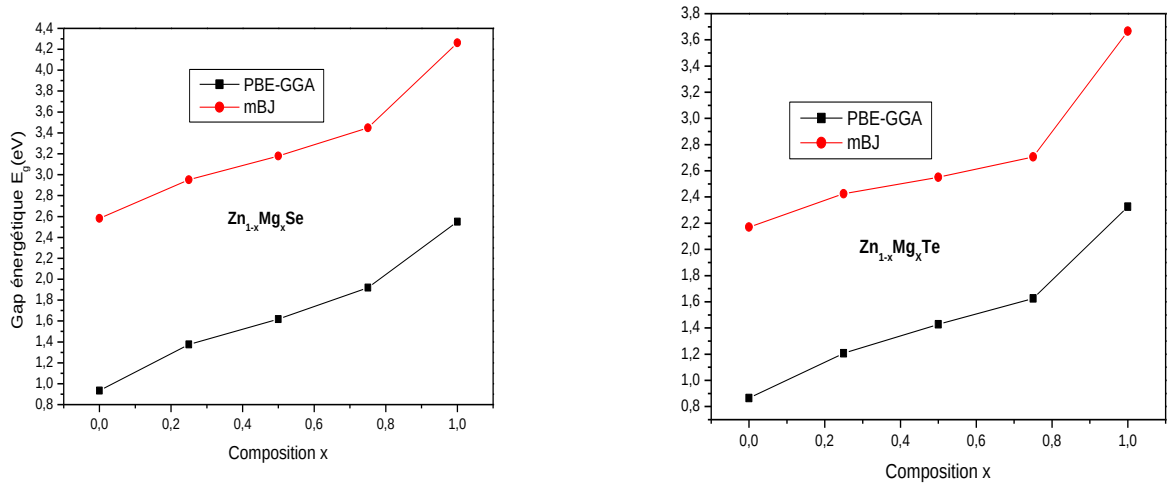

Fig 3 : Variation of energy gaps as a function of concentration for **$ZnSe_yTe_{1-y}$,$MgSe_yTe_{1-y}$, $Zn_{1-x}Mg_xSe$ and $Zn_{1-x}Mg_xTe$** using PBE-GGA and mBJ.

We studied the phase stability **$ZnSe_yTe_{1-y}$,$MgSe_yTe_{1-y}$, $Zn_{1-x}Mg_xSe$ and $Zn_{1-x}Mg_xTe$** alloys by an ab-initio approach **[26,27].** For this reason, we calculate the Gibbs free energy of the alloys ***ΔG_m (x,T)***, which provides access to the phase diagram and thus obtains the critical temperature Tc for the stability of the alloy. The Gibbs free energy for a mixture is given by the expression:

$$\Delta G_m = \Delta H_m - T\Delta S_m \quad \textbf{(3)}$$

Where

$$\Delta H_m = \Omega x(1-x) \quad \textbf{(4)}$$

$$\Delta S_m = -R\left[x\ln x + (1-x)\ln(1-x)\right] \quad \textbf{(5)}$$

ΔHm and ΔSm represent the enthalpy and entropy of the mixture respectively; Ω is the interaction parameter which depends on the considered material; R is the gas constant and T is the absolute temperature. The enthalpy of the alloys is obtained from the total energies calculated for the alloy and the parent binary compounds constituting this alloy. For an ABxC1-x alloy, the enthalpy**ΔHm** is given by:

$$\Delta H_m = E_{AB_xC_{1-x}} - xE_{AB} - (1-x)E_{AC} \quad \textbf{(6)}$$

From the expression (6) ,***ΔH_m/x(1−x)***we can calculate the value of Ω for each concentration from the calculated enthalpies .

By a linear fitting of the curve Ω(x), the expressions of the interaction parameter Ω for the ternary alloys studied are given by the equations:

$$\boldsymbol{ZnSe_yTe_{1-y} \Rightarrow \Omega\left(Kcalmol^{-1}\right) = 2.422x + 10.079} \quad \textbf{(7)}$$

$$\boldsymbol{Zn_{1-x}Mg_xSe \Rightarrow \Omega\left(Kcalmol^{-1}\right) = 4.360x - 0.589} \quad \textbf{(8)}$$

$$\boldsymbol{Zn_{1-x}Mg_xTe \Rightarrow \Omega\left(Kcalmol^{-1}\right) = 5.254x - 2.092} \quad \textbf{(9)}$$

$$\boldsymbol{MgSe_xTe_{1-x} \Rightarrow \Omega\left(Kcalmol^{-1}\right) = 0.902x + 4.932} \quad \textbf{(10)}$$

The average values of Ω(x) in the concentration range 0≤x≤1, obtained from these equations for the alloys **$ZnSe_yTe_{1-y}$,$MgSe_yTe_{1-y}$, $Zn_{1-x}Mg_xSe$ and $Zn_{1-x}Mg_xTe$** are **8.868, 1.591,0.535 and 5.383** kcal/mole, respectively. We calculate the free energy of the mixture $\Delta G_m$for different concentrations using equations **3 and 5**, which will allow us to access the T-x phase diagram. The latter shows the stable, metastable and unstable regions of the alloy. At a temperature lower than the critical temperature TC, the binodal curve is determined for the temperatures verifying the relation

(11)

The spinodal curve is obtained for temperatures obeying $\partial^2(\Delta G_m)/\partial x^2 = 0$.

The phase diagrams obtained for the **$ZnSe_yTe_{1-y}$,$MgSe_yTe_{1-y}$, $Zn_{1-x}Mg_xSe$ and $Zn_{1-x}Mg_xTe$** alloys are shown in **Fig 4**. The observed critical temperature is **525.587, 1020.779, 1075.339 and 2386.87 K$ZnSe_yTe_{1-y}$,$MgSe_yTe_{1-y}$, $Zn_{1-x}Mg_xSe$ and $Zn_{1-x}Mg_xTe$**, respectively. The spinodal curve in the phase diagram marks the equilibrium solubility limit, ie, the miscibility gap. For temperatures above the spinodal curve, ahomogeneous alloy is predicted. The metastable phase is predicted for temperatures lying between the spinodal and binodal curves. Finally, our results indicate that these alloys are stable at high temperature.

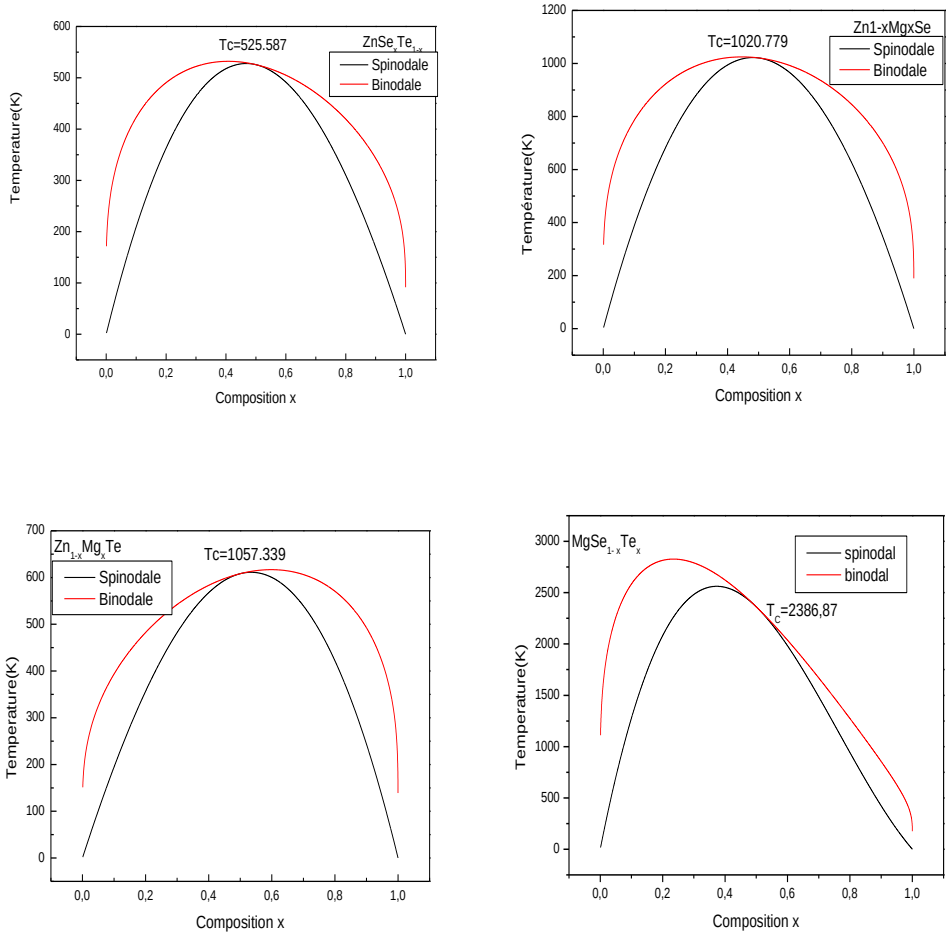

Fig 4: T-x phase diagram of **$ZnSe_yTe_{1-y}$,$MgSe_yTe_{1-y}$, $Zn_{1-x}Mg_xSe$ and $Zn_{1-x}Mg_xTe$** alloys (Dashed line: binodal curve, solid line: spinodal curve).

3.3. Quaternary alloys:

The third step of our work consists in studying the structural and electronic properties of **$Zn_{1-x}Mg_xSe_yTe_{1-y}$** quaternary alloys, to obtain a better understanding of these technologically promising materials. The variations of the lattice parameter, modulus of compressibility and energy gap of the quaternary alloys **$Zn_{1-x}Mg_xSe_yTe_{1-y}$** have been studied as a function of the cationic and anionic compositions (x, y). Lattice parameters, modulus of compressibility and calculated energy gaps of **$Zn_{1-x}Mg_xSe_yTe_{1-y}$** quaternary alloys for different **Mg** and **Se** concentrations are shown in **Table 4**. We have contented ourselves with presenting only our results due to the absence of theoretical and experimental data relating to this quaternary alloy and therefore our results represent a reference for future work on this alloy. **Fig 5 and 6** show the contour of

the lattice parameter and that of the compressibility modulus of **$Zn_{1-x}Mg_xSe_yTe_{1-y}$** respectively. They show the variation of ***a*** and ***B*** as a function of the concentration of selenium y (Se) at different concentrations of magnesium x (Mg) for **$Zn_{1-x}Mg_xSe_yTe_{1-y}$** y. A small deviation of the network constants is visible with respect to Vegard's law. Note also for the compressibility modulus, a small deviation from the linear concentration dependence (LCD) is reported. It can be seen from **Fig 5** that for a given concentration of magnesium Mg, the lattice parameter of the **$Zn_{1-x}Mg_xSe_yTe_{1-y}$** alloy decreases with increasing selenium Se concentration. On the other hand, for a fixed selenium concentration, the lattice parameter increases with increasing magnesium concentration. According to F**ig 6**, we see the increase in the modulus of compressibility with the concentration of **Mg** for ***a*** fixed concentration of selenium. While for a constant concentration of magnesium **Mg**, the modulus of compressibility decreases with the increase in selenium. These behaviors of ***a*** and ***B*** are due to the size difference between the magnesium and selenium atoms.

Table 4: Lattice parameter a_0 and compressibility modulus *B* and energy gap Eg for the quaternary **$Zn_{1-x}Mg_xSe_yTe_{1-y}$.**

x	y	Lattice constant a (Å)	Bulk modulus B (GPa)	E_g (eV) GGA	mBJ
0.25	**0.25**	**6.187**	**42.041**	**1.026**	**2.512**
0.25	**0.5**	**6.074**	**43.517**	**1.189**	**2.610**
0.25	**0.75**	**5.957**	**48.594**	**1.272**	**2.759**
0.5	**0.25**	**6.262**	**38.232**	**1.443**	**2.647**
0.5	**0.5**	**6.248**	**38.894**	**1.447**	**2.775**
0.5	**0.75**	**6.218**	**39.871**	**1.530**	**2.952**
0.75	**0.25**	**6.336**	**37.481**	**1.694**	**2.840**
0.75	**0.5**	**6.218**	**39.871**	**1.721**	**2.999**
0.75	**0.75**	**6.088**	**42.858**	**1.813**	**3.226**

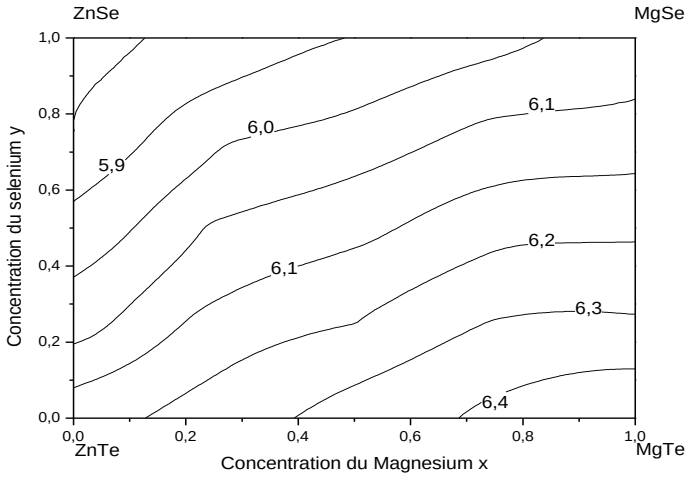

Fig 5: Contour of the lattice parameters a_0 (A°) as a function of the composition x and y of the quaternary alloy **$Zn_{1-x}Mg_xSe_yTe_{1-y}$**

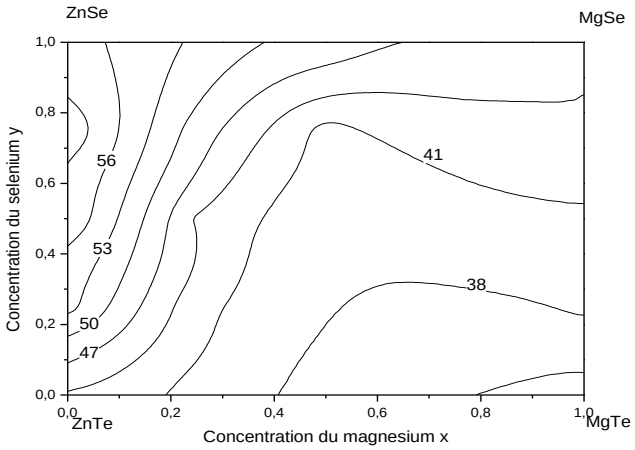

Fig 6: Contour of the compressibility moduli B_0 (GPa) as a function of the composition x and y of the quaternary alloy $\mathbf{Zn_{1-x}Mg_xSe_yTe_{1-y}}$

The energy bands of $\mathbf{Zn_{1-x}Mg_xSe_yTe_{1-y}}$ quaternary alloys were calculated using the two approximations (PBE-GGA) and (mBJ). For all concentrations of x and y, the valence band maximum and conduction band minimum lie at the symmetry point Γ. Therefore, quaternary alloys have a direct gap. Calculation results are presented in **Table 4**. From this table, the largest value of the gap calculated using the mBJ approximation for quaternary alloys is equal to **3.226eV**, which corresponds to **x=y=0.75**. The variation of the values of the energy gaps according to the compositions x and y is illustrated in **Fig 7**. Note that the gaps vary nonlinearly with the compositions and increase with increasing concentrations x and y. The gaps obtained are close to the gaps of the parent binary constituents: **ZnSe, ZnTe, MgSe, MgTe**.

In order to gain some understanding on the interfaces of this alloy, we present the properties of the $\mathbf{Zn_{1-x}Mg_xSe_yTe_{1-y}}$ quaternary alloy adapted to the binary compounds **ZnTe and InAs** taken as semiconductor substrates. We used in our calculations cubic supercells of 64 atoms, where the chosen configuration is the one minimizing the total energy. In a similar way to a ternary, we determined the lattice parameter *a*(x, y) of l quaternary alloy using Vegard's law:

$$a(x,y) = xya_{MgSe} + (1-x)ya_{ZnSe} + x(1-y)a_{ZnTe} + (1-x)(1-y)a_{MgTe} \quad (12)$$

Where a_{ZnSe}, a_{ZnTe}, a_{MgSe} and a_{MgTe} are the lattice parameters of binary compounds. By equalizing the lattice parameter a(x, y) of the quaternary alloy and that of the **ZnTe** then**InAs**substrate (found equal to **6.208A° and 6.05A**° respectively using the **PBE-GGA approximation**) to arrive at the corresponding concentrations **x** and **y** of the quaternary adapted to the two substrates which will have the following forms:

For the **ZnTe** substrate:

$$y = \frac{0.302x}{0.053x+0.455} \quad 0 < x \leq 1 \quad \textbf{(13)}$$

For the InAs substrate:

$$y = \frac{0.302x+0.158}{0?053+0.455} \quad 0 < x \leq 0.78 \quad \textbf{(14)}$$

From the relations **13 and 14** we considered three pairs of different concentrations for each substrate:

ZnTe(x, y) = (1/4, 5/32), (1/3, 7/32), (1/2, 10/32), (1.19/32). **And InAs**(x, y) = (0/32, 11/32), (16/32,

20/32), (20/32,23 /32).

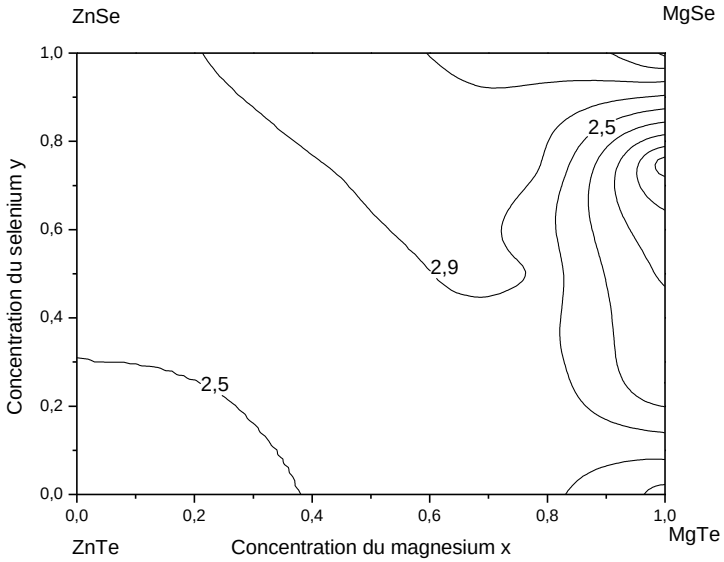

Fig 7: Variation of energy gaps as a function of the x and y compositions of the $Zn_{1-x}Mg_xSe_yTe_{1-y}$ quaternary alloy using mBJ.

In **Figs 8 and 9**, we represent the energy gaps as a function of composition x using the PBE-GGA approximation for **ZnTe** and**InAs** substrates respectively. The gap varies nonlinearly as a function of the concentration x, the bowing factor calculated by the PBE-GGA approximation is relatively low and equal to -0.876 eV for the **InAs**substrate and a significant bowing which is worth **1.976 eV** for the **ZnTe** substrate. The results show that by varying the x and y concentrations in the quaternary alloy adapted to the **ZnTe** and **InAs**substrates, a wide range of gap values is obtained. These results make it possible to obtain new optical properties and thus broaden the field of technological applications and improve the performance of optoelectronic devices. The calculated gap values of $Zn_{1-x}Mg_xSe_yTe_{1-y}$ quaternary alloys adapted to **ZnTe** and **InAs** substrates using the **PBE-GGA** approximation vary from **1.557 to 1.775** eV for the first and **1.485 to 2.471** for the second. The obtained results show that the studied $Zn_{1-x}Mg_xSe_yTe_{1-y}$ quaternary alloys can be used in the design of new laser diodes operating in the blue-green region of the spectrum.

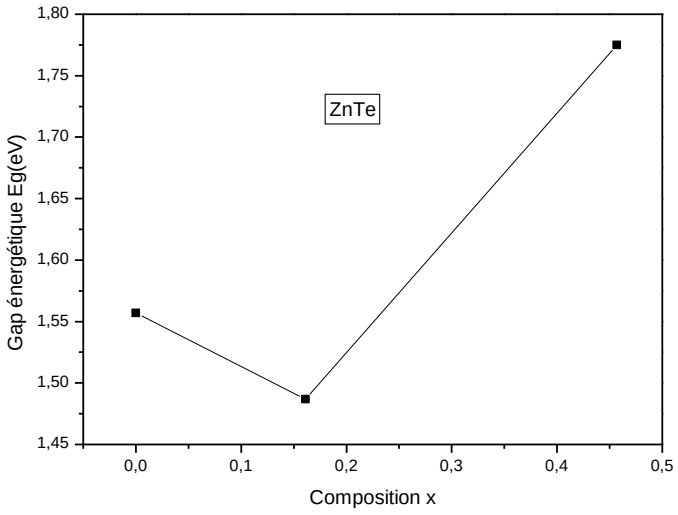

Fig 8: Variation of the energy gap of the $Zn_{1-x}Mg_xSe_yTe_{1-y}$ alloy adapted to the**ZnTe** substrate, as a fuction of the composition x calculated by PBE-GGA Approximation.

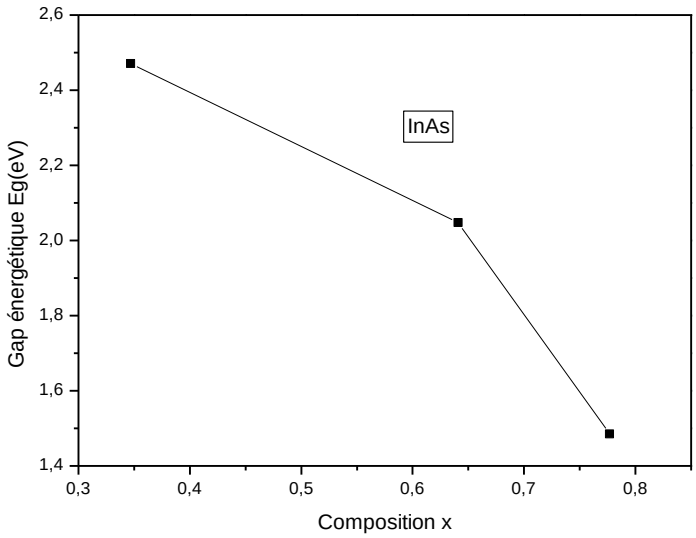

Fig 9: Variation of the energy gap of the **$Zn_{1-x}Mg_xSe_yTe_{1-y}$**alloy adapted to the **InAs** substrate, as a function of the composition x calculated by the PBE-GGA.

4. Conclusion

In summary, we have investigated the structural and electronic properties of **$Zn_{1-x}Mg_xSe_yTe_{1-y}$** quaternary alloys as a function of the compositions x and y by using the FP-LAPW method within **DFT**. Specifically, the lattice constant, bulk modulus and energy band gap, have been calculated. These quantities exhibited non-linear behavior with respect to **x** and **y** compositions. The gap bowing of quaternary alloys is strong at high composition x. Finally, the energy band gap of quaternary alloys **$Zn_{1-x}Mg_xSe_yTe_{1-y}$**lattice matched to **InAs and ZnTe**substrate. The study of these quaternary alloys, our results can be used as reference for future experimental work.

References

[1] L.Bellaiche,S.H.Wei, A.Zunger. Phys.Rev.B54:(1996) 17568.

[2] J. Kapecki, J. Roders, in: M. Howe-Grant (Ed.), Kirk-OthmerEncyclopedia of ChemicaTechnology,fou rth ed., vol. 6(1993), Wiley, NewYork,.

[3] I.Ebbsjö,P.Vashishta,R.Dejus,K.Sköld, J.Phys.C20(1987)L441.

[4] A.Boumaza et al ;. ComputationalMaterials Science 87 (2014) 202–208

[5] J.E.Enderby,A.C.Barnes,Rep.Prog.Phys.53(1990)85.

[6] P.W.Bridgman,ProcAmAcadArtsSci. 74(1945)9.

[7] A.San-Miguel, A. Polian, M. Gauthier, andJ.P. Itié.Rev. B 48: (1993) 8683.

[8] C.J.Pickard, R.J. Needs,NatureMater.9(2010)624.

[9] A.N.Kolmogorov,S.Curtarolo,PhysRevB74(2006)224507.

[10] J.Feng,R.G. Hennig,N.W. Ashcroft,R. Hoffmann,Nature (2008)445.

[11]D.S.Sofronov,Y.A.Zagoruiko,N.O.Kovalenko,A.S.Gerasimenko,V.N.Baumer,P.V.Mateychenko,showall.Vol28,(2013)944

[12] J.C. Guillaume, J. Chevallier, J.F. Rommeluere, G. Rouy, G. Revel. Rev.Phy. App.11(1976)725 .

[13] CrystalGrowthofZnSexTe1-xSolidSolutions.Jap.J.Phy.App.12(1973)232.

[14] Anderson OK. Linear methods in band theory. Phys Rev B. 1975;12:3060–3083.

[15] Hohenberg P, Kohn W.

Inhomogeneous electron gas. Phys Rev. 1964;136:864–871

[16] Kohn W, Sham LJ. Self-consistent equations including exchange and correlation effects. Phys Rev A. 1965;140: A1133.

[17] Blaha P, Schwarz K, Madsen GKH, et al. WIEN2K, an augmented plane wave plus local orbitals program for calculating crystal properties (2008). Vienna;.

[18] Wong KM, Alay-e-Abbas SM, Fang Y, et al.. J Appl Phys. (2013);114:034901.

[19] Perdew JP, Burke S, Ernzerhof M. Generalized gradient approximation made simple. Phys Rev Lett. (1996);77:3865–3868

[20] Tran F, BlahaP..Phys Rev Lett. 2009;102:226401–226405

[21] F.D. Murnaghan, Proc. Natl.Acad. Sci. USA 30 (1944) 5390.

[22] Vegard L, Z. Phys. (1921). 5-17

[23] J.H. Chang, M. W. Cho, H. Makino, T. Sekiguchi and T.Yao J. Kor.Phys. 1999 ; 34 :980-8577

[24] K. Watanabe et al. J. Appl. Phys. (1997). **81**, 451

[25] D.J. Chadi, Phys. Rev. Lett. (1994) **72**,534.

[26] R.A. Swalin,Thermodynamics*(*1961).of Solids(New York: Wiley).

[27] L.K. Teles, J. Furthmuller,L.M.R.Scolfaro, J.R. Leite and F. Bechstedt,*Phys. Rev*(2000).. B 62. 2475

[28] R. Franco, P. Mori-Sánchez, J. M. Recio, and R. Pandey, Phys.(2003) Rev. B 68, 195208.

[29] S.-G. Lee and K. J. Chang, Phys.(1995) Rev. B 52, 1918.

[30] O. Madelung (Ed.), ,Landolt Bo rnstein, New Series Group III, vol. 17, Springer-Verlag, Berlin, 1982.

[31] W. M. Yim, J. P. Dismukes, E. J. Stofko, and R. J. Poff, J. Phys. (1972) Chem. Solids 33, 501.

[32] F.E. Haj Hassan, H. Akbarzadeh. Computational Materials Science 35 (2006) 423–431.

[33] K. Hacini, H. Meradji, S. Ghemid and F. El Haj Hassan (2012) Chin. Phys. B Vol. 21, No. 3. 036102.

[34] A. Berghout, A. Zaouib and J. HugelSuperlattices and Microstructures 44 (2008) 112–120.

[35] O. Madelung (ed.), Londolt-Börnstein New Series III, Springer, Berlin, (1987), Vol. 22.

[36] Fleszar A. LDA, GW, and exact-exchange Kohn-Sham scheme calculations of the electronic structure of sp semiconductors. PhysRev B. 2001;64:245204.

[37] Jobst B, Hommel D, Lunz U, et al. E0 band_gap energy and lattice constant of ternary Zn1-xMgxSe as functions of composition. ApplPhys Lett. 1996;69:97–99.

[38] Watanabe K, Litz MT, Korn M, et al..J Appl Phys. 1997;81:451–455.

[39] H. Baaziz, Z. Charifi, F. El Haj Hassan, S. J. Hashemifar, and H. Akbarzadeh, phys. (2006) stat. sol. (b) 243, 1296.

[40] H. Okuyama, Y. Kishita, and A. Ishibashi, Phys. Rev. B 57, (1998) 2257–2263.

[41] El Haj Hassan F, Amrani B and Bahsoun F (2007) Physica B 391-365.

[42] A. M. Saitta, S. de Gironcoli, and S. Baroni, Appl. Phys. Lett. 75, 2746 (1999).

[43] X. Liu and J. K. Furdyna, J. Appl. Phys. (2004). 95, 7754.

[44] L.D. Landau, E.M. Lifshitz, Electrodynamics in Continuous Media, Pergamon Press, Oxford, (1960).

[45] Z. Charifi, F. El Haj Hassan, H. Baaziz, Sh. Khosravizadeh, S.J. Hashemifar and H. Akbarzadeh, J. Phys.: Condens Matter 7 (2005) 7077.

[46] Waag A, Heinke H, Scholl S, Becker CR, Landwwehr G. Growth of MgTe and $Cd_{1-x}Mg_xTe$ thin films by molecular beam epitaxy. J. Cryst. Growth. 1993; 131: 607-611.